Therapeutic benefits of a component of coffee in a rat model of Alzheimer's disease

Gustavo Basurto-Islas [a,1], Julie Blanchard [a], Yunn Chyn Tung [a], Jose R. Fernandez [b], Michael Voronkov [b], Maxwell Stock [b], Sherry Zhang [c], Jeffry B. Stock [b,c], Khalid Iqbal [a,*]

[a] Department of Neurochemistry, New York State Institute for Basic Research in Developmental Disabilities, Staten Island, NY, USA
[b] Signum Biosciences Inc, 133 Wall Street, Princeton, NJ 08540, USA
[c] Department of Molecular Biology, Princeton University, Princeton, NJ, USA

ABSTRACT

A minor component of coffee unrelated to caffeine, eicosanoyl-5-hydroxytryptamide (EHT), provides protection in a rat model for Alzheimer's disease (AD). In this model, viral expression of the phosphoprotein phosphatase 2A (PP2A) endogenous inhibitor, the I_2^{PP2A}, or SET protein in the brains of rats leads to several characteristic features of AD including cognitive impairment, tau hyperphosphorylation, and elevated levels of cytoplasmic amyloid-β protein. Dietary supplementation with EHT for 6–12 months resulted in substantial amelioration of all these defects. The beneficial effects of EHT could be associated with its ability to increase PP2A activity by inhibiting the demethylation of its catalytic subunit PP2Ac. These findings raise the possibility that EHT may make a substantial contribution to the apparent neuroprotective benefits associated with coffee consumption as evidenced by numerous epidemiologic studies indicating that coffee drinkers have substantially lowered risk of developing AD.

© 2014 Elsevier Inc. All rights reserved.

1. Introduction

Alzheimer 's disease (AD), the major cause of dementia in middle and old age, is characterized by neurodegeneration that is associated with neurofibrillary tangles and neuritic plaques. A current major goal in medicine is the development of disease-modifying therapeutic drugs for AD. The microtubule-associated tau protein is abnormally hyperphosphorylated in AD where it is the principle component of neurofibrillary tangles (Bancher et al., 1989; Grundke-Iqbal et al., 1986a, 1986b). Similarly, the amyloid-β (Aβ) polypeptide, is the principle component of neuritic plaques (Masters et al., 1985; Wong et al., 1985). Evidence suggests that tangle and plaque precursors, the nonfibril forms of abnormally hyperphosphorylated tau and soluble oligomers of Aβ, are the major cytotoxic species in AD (Alonso et al., 1994, 2010; Grundke-Iqbal et al., 1989; Iqbal et al., 1986; Klein, 2002; Kopke et al., 1993; Santacruz et al., 2005). As much as 40% of the abnormally hyperphosphorylated tau is cytosolic in AD brains (Kopke et al., 1993), and intraneuronal Aβ accumulation precedes plaque deposition (Bancher et al., 1989; Cataldo et al., 2004; Grundke-Iqbal et al., 1989; Mori et al., 2002) and is correlated with neuronal cell death in AD transgenic mouse models (Espana et al., 2010; Gandy et al., 2010; Oddo et al., 2003).

Phosphoprotein phosphatase 2A (PP2A) accounts for ∼70% of the total phospho-tau phosphatase activity in healthy human brain (Bennecib et al., 2000; Gong et al., 1993, 1995, 2000; Liu et al., 2005) and also functions to dephosphorylate the Aβ precursor protein (APP) so as to reduce the formation of the Aβ (Sontag et al., 2007). In

AD, PP2A activity is curtailed so that levels of hyperphosphorylated tau and Aβ increase, leading to neurodegeneration and dementia (Gong et al., 1993). Two cellular inhibitor proteins, I_1^{PP2A} and I_2^{PP2A}, regulate the activity of PP2A (Li et al., 1995, 1996). I_2^{PP2A} or SET inhibits PP2A activity toward hyperphosphorylated tau (Tsujio et al., 2005). I_2^{PP2A} is a 277 amino acid–long nuclear protein that is overexpressed and selectively cleaved at N175 into N-terminal (I_{2NTF}) and C-terminal (I_{2CTF}) fragments, which are translocated from the neuronal nucleus to the cytoplasm in affected areas of the AD brain (Tanimukai et al., 2005). Both I_{2NTF} and I_{2CTF} bind to PP2A catalytic subunit (PP2Ac) and inhibit its phosphatase activity toward hyperphosphorylated tau (Arnaud et al., 2011). Transduction of brains of new born rat pups with adenoassociated virus 1 vector (AAV1) encoding I_{2NTF} and I_{2CTF} inhibit PP2A activity and cause abnormal hyperphosphorylation and aggregation of tau and accumulation of intraneuronal Aβ in 13-month-old animals (Bolognin et al., 2012). These protein hallmarks of AD are associated with cognitive defects in memory and learning.

From these results, it seems likely that a therapeutic agent that acts to maintain healthy levels of PP2A might provide a disease-modifying approach for the treatment of AD. A number of different PP2A-activating compounds and mechanisms have been identified (Voronkov et al., 2011). An in vitro screen was conducted for natural products that support PP2A activity toward phospho-tau, and a suitable activity was identified in coffee extracts. The active agent was purified to homogeneity and identified as eicosanoyl-5-hydroxytryptamide (EHT). Synthetic EHT exhibited the same ability to support PP2A activity as EHT isolated from coffee. Dietary supplementation with synthetic EHT exhibited neuroprotective efficacies in mouse models for Parkinson's disease (Lee et al., 2011, 2013). Here, we report the beneficial effects of chronic dietary supplementation with EHT on PP2A activity, abnormal tau hyperphosphorylation, accumulation of intraneuronal Aβ, and cognitive performance in a rat model for AD.

2. Materials and methods

2.1. Study design

AAV1 was used to express the I_2^{PP2A} N- and C-terminal fragments (I2-N/C) in rat brain to replicate the cleavage of I_2^{PP2A} found previously in AD brains (Tanimukai et al., 2005). AAV1-I2-N/C–infected rats that express the predicted I2-N/C fragments, are cognitively impaired, show hyperphosphorylation and aggregation of tau, and accumulate intraneuronal Aβ (Bolognin et al., 2012). As described previously (Bolognin et al., 2012), on the day of birth (postnatal day = 0.05), Wistar rat pups were transfected by injecting 2 μL containing 4×10^9 AAV1 genomic equivalents encoding I2-N/C or, as a control, green fluorescent protein (GFP) into each lateral ventricle of the brain (Fig. 1). Successful transfection of rat brains with I2-N/C was confirmed by reverse-transcription polymerase chain reaction (RT-PCR). At 21 days of age, the pups were weaned and 15 female AAV1-I2-N/C and 15 female AAV1-GFP rats were put on 0.1% (wt/wt) EHT formulated diet (Research Diets; New Brunswick, NJ, USA). As controls, 15 female AAV1-I2-N/C and 15 female AAV1-GFP pups were put on similar diets lacking EHT. The rats were housed and bred according to the United States Public Health Service Policy on Human Care and Use of Laboratory animals with 2–3 animals per cage, a 12:12 h light-dark cycle, and ad libitum access to food and water. Studies on animals were carried out according to the protocols approved by the Animal Welfare Committee of the New York State Institute for Basic Research. Rats were subjected to behavioral tests at 6 months of age. Seven animals from each group were perfused after behavioral tests, and the remaining 8 animals from each group were perfused after a second set of behavioral tests at 12 months while they were still on EHT or vehicle diet. Animals were anesthetized with sodium pentobarbital (125 mg/kg) and then sacrificed by transcardial perfusion with 0.1 M phosphate-buffered saline. The left hemispheres were dissected into hippocampus, cerebral cortex,
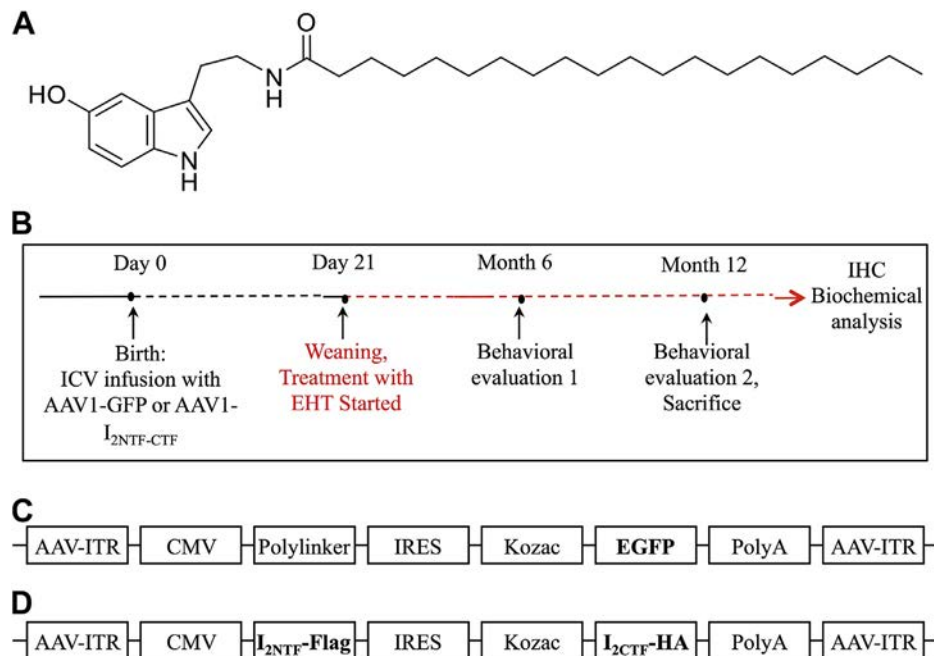
Fig. 1. Eicosanoyl-5-hydroxytryptamide (EHT) structure and experimental design and I_2^{PP2A} N- and C-terminal fragments (I2-N/C) transduction in adult rat brains. (A) EHT chemical structure. (B) Schematic representation of the study. (C) Rat pups were injected intracerebroventricularly with adenoassociated virus (AAV) on the day of birth. (D) Linear maps of the AAV plasmids (based on pTRUF12) containing (C) green fluorescent protein (GFP) or (D) I_{2NTF} and I_{2CTF} genes inserted between the inverted terminal repeats (ITRs). CMV, cytomegalovirus promoter; IRES, internal ribosomal entry site from poliovirus. After weaning on day 21, GFP and I2-N/C animals were put on either standard rat chow or chow containing 0.1% EHT for up to 1 year.

and subcortical structures and kept at $-80\ °C$ for biochemical analysis, whereas for immunohistochemical investigation, the right hemispheres were immerse-fixed for 48 hours in 4% paraformaldehyde in phosphate-buffered saline, cryoprotected in 30% sucrose, and then cut in 40 μm sagittal sections using a freezing-sliding microtome.

2.2. Recombinant plasmid production and vector packing

AAV1-I$_2$-N/C and AAV1-GFP were generated as described previously (Bolognin et al., 2012; Wang et al., 2010). Briefly, the plasmid pEGFP $-$ N3/I$_2^{PP2A}$ (Tsujio et al., 2005) was used as a template to generate by PCR I$_2$-N/C encoding complementary DNAs (cDNAs). After verification by DNA sequencing, the cDNA fragments were cloned into the multicloning site of the AAV viral genome containing plasmid pTRUF12. Expression was driven by the cytomegalovirus promoter/enhancer. Serotype 1 virus was produced (Henckaerts et al., 2009), and titers were calculated from standard curves generated from pTRUF12 as previously described (Zolotukhin et al., 2002).

2.3. Western blots

Rat hippocampus was homogenized to 10% (wt/vol) final concentration in cold buffer containing 50 mM Tris-HCl (pH 7.4), 8.5% sucrose, 2 mM EDTA, 2 mM EGTA, 10 mM β-mercaptoethanol, 5 mM benzamidine, 0.5 mM AEBSF, 4 μg/mL pepstatin A, 10 μg/mL each of aprotinin and leupeptin, 20 mM β-glycerophosphate, 100 mM sodium fluoride, 1 mM sodium vanadate, and 100 nM okadaic acid (OA). Protein concentrations were determined by the modified Lowry method (Bensadoun and Weinstein, 1976). Tissue homogenates were heated in Laemmli buffer and subjected to sodium dodecyl polyacrylamide gel electrophoresis. Proteins were transferred to polyvinylidine difluoride membrane of 0.45 μm pore size, and membranes were blocked with 5% nonfat dry milk. The following primary antibodies were used: anti-glyceraldehyde 3-phosphate dehydrogenase (1:2000; Santa Cruz Biotechnology, Santa Cruz, CA, USA); 92e to total tau (1:5000; Grundke-Iqbal et al., 1988); and phosphospecific tau antibodies tau pS199, tau pT205, tau pT212, tau pS214, tau pS396 (1:1000; BioSource, Camarillo, CA, USA), R145 to tau pS422 (1:3000, Tanaka et al., 1998), 12E8 to tau pSer396/Ser404 (1:500, Seubert et al., 1995), 4D9 to methyl-PP2A (1:200; Princeton University, NJ, USA), 1D6 to unmethylated PP2A (Millipore), and 6A3 to total PP2A (Millipore). Immunoblots were probed with the corresponding anti-mouse or anti-rabbit horseradish peroxidase secondary antibodies (1:5000; Jackson ImmunoResearch, West Grove, PA, USA) and detected using enhanced chemiluminescence reagents (Thermo Scientific, Rockford, IL, USA). Multi-Gauge V3 software (Fuji Photo Film, Tokyo, Japan) was used to quantify the density of the protein bands in Western blots. The quantified values were statistically analyzed with the nonparametric t test.

2.4. RT-PCR and quantitative PCR

Total RNA was extracted from cerebral cortex, with RNeasy plus mini kit (Qiagen, Valencia, CA, USA) according to the manufacturer's instructions. cDNA synthesis was performed using Super Script First-Strand Synthesis System kit (Invitrogen, Carlsbad, CA, USA). RT-PCR amplification was achieved in a thermocycler for 30 cycles: denaturation for 30 seconds at 95 °C, annealing for 30 seconds at 60 °C, and polymerization for 30 seconds at 72 °C. The I$_2^{PP2A}$ N-terminal-FLAG primer sequence was the following: forward 5′-gcaagaagcgattgaacaca-3′ and reverse 5′-gcagtgcctcttcatcttcc-3′. The

amplification products were resolved on 1% agarose gels and quantified using the Molecular Imager System (Bio-Rad, Hercules, CA, USA).

2.5. Immunohistochemistry

Immunohistochemistry was performed on free-floating cryostat sagittal sections of right-brain hemispheres. The following antibodies were used at the indicated dilution: anti-Aβ$_{1-40}$ (1:200; Invitrogen, Camarillo, CA, USA) and Alexa 555−conjugated goat anti-mouse and goat anti-rabbit IgG (H + L) (1:500; Molecular Probes, Carlsbad, CA, USA) were used as secondary antibodies. Sections were analyzed using confocal microscope Nikon eclipse 90i (Nikon, Melville, NY, USA). For quantitative analysis, the images were taken using ×10 objective, 6 images into 5 μm depth through the z axis were scanned, and horizontal z sections were collected and projected as superimposed stacks. The antibody staining was semiquantitated by measuring mean fluorescence intensities (MFIs) with Image J software (US National Institutes of Health, Bethesda, MD, USA). MFI per square micrometer area was calculated by dividing the MFI units by the area of outlined regions. The CA3 region from 4 sections per brain and 4 animals per group were used for fluorescence intensity and quantification of Aβ$_{1-40}$.

2.6. PP2A activity assay

PP2A activity toward phospho-tau was assayed as described previously (Chohan et al., 2006). Briefly, 96-well plates were coated for 8 hours at room temperature with 60 μL of 35 mM NaHCO$_3$ pH 9.5, containing 8.0 μg/mL of a synthetic tau phosphopeptide in which Ser199 was phosphorylated. The coating solution was removed, and the wells were blocked with 150 μL of protein-free blocking buffer (Pierce, Pittsburgh, PA, USA) at 4 °C overnight and then washed with 50 mM Tris-HCl, pH 7. Phosphatase activity was assessed with 60 μL per well of 0.15 μg tissue extract (prepared with protease but no phosphatase inhibitors) resuspended in reaction buffer (20 mM β-mercaptoethanol, 2 mM EGTA, 2 mM MnCl$_2$, and 0.01 mg/mL bovine serum albumin) in the presence or absence of 20 nM OA for 60 minutes at 30 °C in a moist chamber. Each well was then incubated overnight at 4 °C with 75 μL of a monoclonal antibody, tau-1 (1:25,000), specific for tau that is unphosphorylated at Ser-198/199/202 (Grundke-Iqbal et al., 1986b). Plates were developed with anti-mouse horseradish peroxidase secondary antibody (1:5000; Jackson ImmunoResearch) and tetramethylbenzidine. Development was monitored in a microtiter plate reader at 650 nm with a 30-minute kinetic reading every 2 minutes. To determine PP2A activity, values in the presence of OA were subtracted from the corresponding values in the absence of OA.

2.7. Behavioral studies

Once a week, the condition of each animal was assessed by measuring body weight, rectal temperature, food consumption, grooming, physical state, and clasping reflex. After 6 and 12 months of treatment, animals were subjected to hippocampal-dependent spatial memory tests using the water maze and object location, respectively. All the behavior procedures on animals were conducted in strict compliance with approved protocols from our institutional Animal Welfare Committee.

2.8. Spatial reference memory evaluation at 6 months

The spatial reference memory task evaluated in a water maze assesses hippocampal-dependent reference memory in rodents, requiring that rats use a spatial navigational strategy to find a fixed

submerged escape platform. The hippocampal system processes information about the relationships among distal environmental cues into a spatial map where spatial coordinates of the submerged platform are encoded (Morris et al., 1982). The hippocampus is also crucial for memory storage, consolidation, and restitution of the spatial information (Riedel et al., 1999). The procedure was performed in a 180-cm diameter circular tank. The pool was filled with water (20 $\pm$ 1 °C) made opaque by adding white nontoxic paint. Acquisition was started with the escape platform (14 cm diameter submerged 1 cm below water surface) in the northwest quadrant, and each animal was given 90 seconds to find the platform. If the rat did not find the platform in 90 seconds, it was gently guided to it. At the end of each trial, the rat was left on the platform for 20 seconds, dried, and then returned to its home cage until the next trial. Four such acquisition trials, 20 minutes apart, were given on each day for 3 consecutive days. A test for retention (i.e., a probe trial [PT]) was given 24 hours after the last day of training. During the PT, the rat was allowed to swim in the tank without the escape platform for 60 seconds. The measures of learning were the time and the distance swum to reach the virtual escape platform. For PT, the number of entries in the platform zone was recorded. Rat behavior in the water maze was monitored by a Samsung digital camera (SDC 4304) mounted to the ceiling and tracked and timed by SMART (PanLab/San Diego Instruments) version 2.0.14 software.

2.9. Object location evaluation

This task was performed after 12 months of treatment and was used to measure hippocampal functioning because this brain structure is critical for associating objects with locations (Malkova and Mishkin, 2003). Animals were exposed to 2 similar objects and they had to identify the spatial location of these 2 objects in an open field as novel or familiar, based on the memory of an earlier experience with one of the 2 different object locations. The familiar location was explored a shorter time than the novel location because the spatial representation of the former was still available in the memory. The test was developed in the classical open-field apparatus (i.e., a polyvinyl chloride square arena, 100 × 100 cm, with plexiglass walls, 70 cm high). The open field was placed in a different room from the experimenter. The open field was surmounted by a video camera connected to a computer for tracking. Before the object location test, animals received 6 sessions of habituation to the arena (2 session per day, 2 hours apart, 10 minute per session). During habituation sessions, an object was placed in the center of the arena. During the first habituation session, the time of exploration of the object was measured to evaluate neophobia. Twenty-four hours after the last session of habituation, rats performed the object location test consisting of a sample phase and a test phase. During the sample phase, the rat was exposed to 2 similar objects and was allowed to explore for 5 minutes. The test phase occurred 1 hour after the sample phase. One of the 2 identical objects was moved to a new location. To analyze cognitive performance, a discrimination index was calculated as follow: (time exploring the new location − time exploring familiar location) × 100/time exploring both locations. Rat behavior in the open field was monitored by a Samsung digital camera (SDC 4304) mounted to the ceiling and tracked and timed by SMART (PanLab/San Diego Instruments) version 2.0.14 software. Time spent close to each object was manually recorded by the experimenter.

2.10. General behavioral studies: monitoring of animals

During the period of the treatment, the individual condition of each animal was assessed every week by evaluating grooming and physical state and by measuring body weight, rectal temperature, and food consumption.

2.11. Anxiety

Anxiety and exploratory activities were evaluated after 6 months of treatment with EHT by allowing rats to freely explore an open field for 20 minutes. The testing apparatus was a classic open field (i.e., a polyvinyl chloride square arena of 100 × 100 cm, with 70 cm high plexiglass walls). The open field was placed in a part of the room separated from the experimentator and the control station with a black opaque curtain. Rats were individually submitted to a single 20-minute session. Because for rodents the middle of a nonfamiliar arena is anxiogenic, anxiety was studied analyzing the time spent in the middle of the arena during the first 5 minutes of the session. To assess exploratory activity, the total distance the animals covered in the arena was tracked and measured. Data collection was performed using tracking files of the experiment recorded with SMART (PanLab/San Diego Instruments) version 2.0.14 software.

2.12. Neurologic evaluation

After the first 6 months of treatment, rats were submitted to a battery of behavioral tests to perform a quantitative evaluation of reflexes, muscle strength, and motor coordination. Using a scoring system adapted from Korenova et al. (2009), we were able to measure the consequences of the neurodegenerative processes on neurologic and neuromuscular functions (see Supplementary Table S1).

2.12.1. The beam-walking test
Three sorts of traversing segments were used (3 × 3 cm, 4 × 2 cm [traversing segment was 2 cm], and a round beam of 3.5 cm diameter). All had the same length of 200 cm and were placed 75 cm above the floor. Two training and 1 testing trials were performed. Traversing latency and number of hind-limb slips made during test performance were measured and scored according to the predefined rating scale (Supplementary Table S1). The task was repeated at different sensitivity according to the following scheme:

- beam with a square section of 3 × 3 cm (day 1),
- beam with a rectangular cross-section of 4 × 2 cm (day 2), and
- beam with a round cross-section of 3.5 cm diameter (day 3).

2.12.2. The prehensile traction test
Rats were allowed to grasp with their forepaws a horizontal steel wire (3 mm in diameter) suspended 75 cm above a padded surface. Latency to fall from the wire was measured. The scoring conditions are described in Supplementary Table S1.

After 12 months of treatment, neurologic functions were evaluated using a test for neuromuscular functions (i.e., the hind-limb extension reflex test), a test for muscle strength (i.e., the prehensile traction test), and a test for motor coordination (i.e., the footprint test).

2.12.3. The hind-limb extension reflex test
The test measures the consequences of the neurodegenerative processes on neurologic and neuromuscular functions. The scoring conditions are described in Supplementary Table S2.

2.12.4. The prehensile traction test
The test evaluates forelimb muscle strength. Rats were allowed to grasp with their forepaws a horizontal steel wire (3 mm in

diameter) suspended 75 cm above a padded surface. Latency to fall from the wire was measured. The scoring conditions are described in Supplementary Table S3.

2.12.5. The footprint test

The test evaluates motor coordination and synchrony by examining gait during normal walking. For this test, the animal paws are stained with nontoxic acrylic paint (forepaws with red and hind paws with blue). The rat has to walk through a $12 \times 12 \times 50$ cm transparent plexiglass tunnel over absorbent paper. The following records were made from the walking tracks (see Supplementary Fig. S1): (1) stride length (distance between forepaw-forepaw and hind paw-hind paw), (2) gait width (distance between left and right hind paws), and (3) placement of hind paw relative to forepaw (distance between hind paw-forepaw in each step cycle).

3. Results

3.1. I_{2NTF} and I_{2CTF} genes were effectively expressed in rat brains

Rat pups were injected intracerebroventricularly on the day of birth with AAV1 containing N- and C-terminal fragments of the PP2A inhibitor, $I_2^{PP2A}(I_2 - N/C)$ or as control, AAV1-GFP, and after weaning on day 21, GFP and I_2-N/C animals were put on either standard rat chow or chow containing 0.1% EHT for up to 1 year (Fig. 1). As shown previously (Bolognin et al., 2012), considering an FLAG-tag was encoded into the I_2^{PP2A} N-terminal fragment sequence, we were able to use I_2^{PP2A} N-terminal fragment primers that contain an FLAG sequence not homologous to endogenous I_2^{PP2A} to confirm the successful transduction of the brain with the AAV1-I_2-N/C. The AAV1-mediated protein expression was <5% of the endogenous I2PP2A level as reported previously (Wang et al., 2010). As expected, FLAG-tagged I_2^{PP2A} N-terminal fragment sequences were not found in GFP control rats.

3.2. EHT prevents I_2-induced cognitive impairment in rats

The expression in rat brains of the highly active N- and C-terminal fragments of the PP2A inhibitor, $I_2^{PP2A}(I_2 - N/C)$, led to cognitive deficits, and dietary supplementation with EHT relieved these deficiencies (Figs. 2 and 3). Hippocampal-dependent cognitive function was assessed at 6 months using the spatial reference memory task in the water maze (Fig. 2). Analysis of the swim speeds of the animals (Fig. 2A) revealed that AAV-I_2-N/C rats swam significantly faster than other groups, independent of EHT supplementation (analysis of variance [ANOVA], $p = 0.003$; Fisher post hoc test, $p < 0.049$). Results of the training were therefore analyzed in terms of distance covered to reach the submerged platform rather than time required (Fig. 2B). During training in the absence of EHT dietary supplementation, AAV-I_2-N/C rats displayed delayed performance compared with other groups (Fig. 2B, ANOVA, $p = 0.038$; Fisher post hoc test, $p < 0.046$). This finding showed that AAV-I_2-N/C rats were impaired in the learning of the task compared with AAV-GFP rats, but that treatment with EHT rescued this impairment. During the PT, AAV-I_2-N/C rats also displayed poor performance and visited the platform location significantly less frequently than AAV-GFP rats raised on control diets lacking EHT (Fig. 2C, Student t test, $p = 0.023$). This confirmed the impaired ability of AAV-I_2-N/C rats to encode and memorize spatial information, that is, the spatial coordinates of the submerged platform. The AAV-I_2-N/C rats treated with EHT visited the platform location similarly to the AAV-GFP control animals, confirming that treatment of AAV-I_2-N/C rats with EHT prevented spatial memory impairment.

After 12 months of EHT treatment, hippocampal cognitive function was evaluated using a different test: the object location memory task. During the sample phase of the test, all animals spent similar time exploring the 2 objects in the arena (Fig. 3A, Student t test, $p > 0.999$). This result shows that the rat's baseline preferences for the objects and locations involved in the test were not significantly affected by I_2-N/C expression or EHT dietary supplementation. During the test phase, control groups and AAV-I_2-N/C rats treated with EHT displayed a discrimination ratio of $\sim 70\%$ showing that these animals tend to explore the new location more than the old. In contrast, AAV-I_2-N/C rats that were not treated with EHT presented a discrimination ratio close to 55%, showing that this group spent similar time in both locations. The performance of this group was statistically different from control and EHT-treated groups (Fig. 3B, Student t test, $p < 0.020$). These results confirmed the hippocampal impairment associated with AAV-I_2-N/C expression seen at 6 months in the water-maze task and showed that 12 months of EHT treatment can prevent the impairment of spatial information processing associated with I_2-N/C expression.
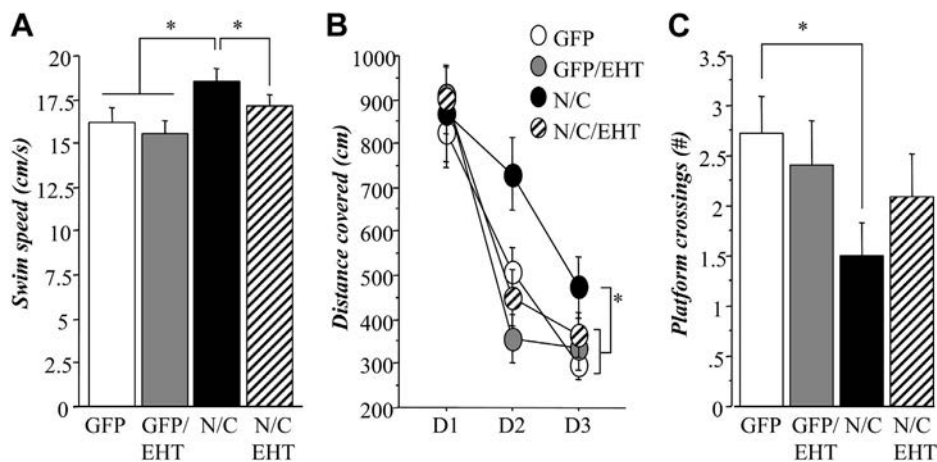

Fig. 2. Eicosanoyl-5-hydroxytryptamide (EHT) prevents the reference memory impairment in rats expressing I_2^{PP2A} N- and C-terminal fragments (I_2-N/C) when tested by the hippocampal-dependent spatial memory water-maze test. (A) Hippocampal functioning in I_2-N/C rats displayed significantly faster swim speed than other groups (analysis of variance [ANOVA], $p < 0.01$; Fisher post hoc test, $p < 0.05$); therefore, results of the training phase were analyzed as distance covered to reach the submerged platform. (B) Water-maze task: training phase. I_2-N/C rats treated with vehicle displayed delayed training performance compared with other groups (ANOVA, $p = 0.038$; Fisher post hoc test, $p < 0.046$) reflecting hippocampal impairment that can be prevented with 6 months treatment with EHT. (C) Water-maze task: probe trial. I_2-N/C rats treated with vehicle visited the platform location less than other groups (Student t test, $p = 0.023$), confirming hippocampal impairment and its prevention by 6 months treatment with EHT. $^*p < 0.05$.
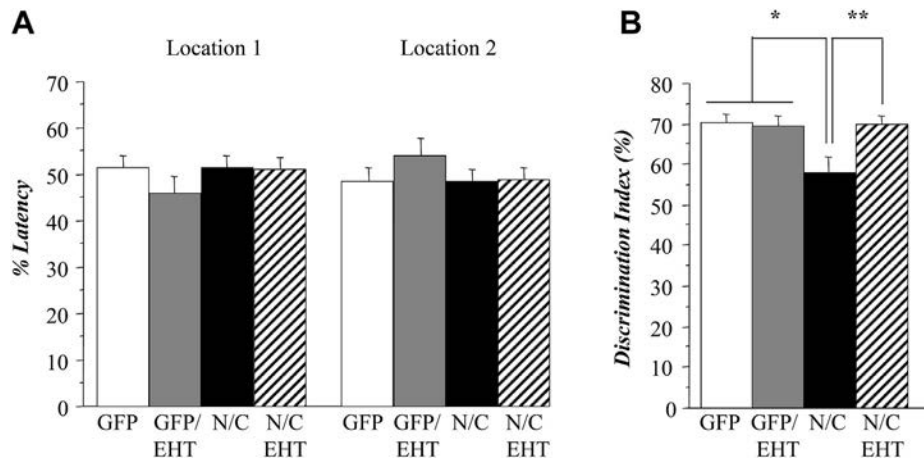
Fig. 3. Eicosanoyl-5-hydroxytryptamide (EHT) prevents the cognitive impairment in rats expressing I_2^{PP2A} N- and C-terminal fragments (I_2-N/C). Hippocampal functioning was measured to determine cognitive impairment. (A) Object location task: sample phase. No differences were found among the groups, indicating no preferences for objects or location (Student t test, $p > 0.99$). (B) Object location task: test phase. I_2-N/C rats spent significantly less time to analyze the object in the new location (Student t test, $p < 0.02$), indicating cognitive impairment. When treated with EHT for 12 months I_2-N/C rats displayed similar performance as control groups. Abbreviation: GFP, green fluorescent protein. $^*p < 0.05$, $^{**}p < 0.01$.

3.3. General physical state, body weight, and temperature

No alteration in general physical state including grooming and posture because of either the AAV-$I_{2NTF/CTF}$ (N/C/vh) infection or the treatment with EHT was detected. Figure 4 represents the follow-up of body weight and body temperature during the treatment with EHT (Fig. 4A and C, during the first 6 months;

Fig. 4B and D, during the last 6 months). Across months, we observe a general increase of the body weight (Fig. 4A and C, ANOVAs, $p < 0.001$) and of the body temperature (Fig. 4C and D, ANOVAs, $p < 0.001$). But, we did not observe any significant effect of AAV-$I_{2NTF/CTF}$ infection or EHT on these parameters (Fig. 4A and C, ANOVAs, $p > 0.141$; Fig. 4B and D, ANOVAs, $p > 0.263$) during the period of the treatment.
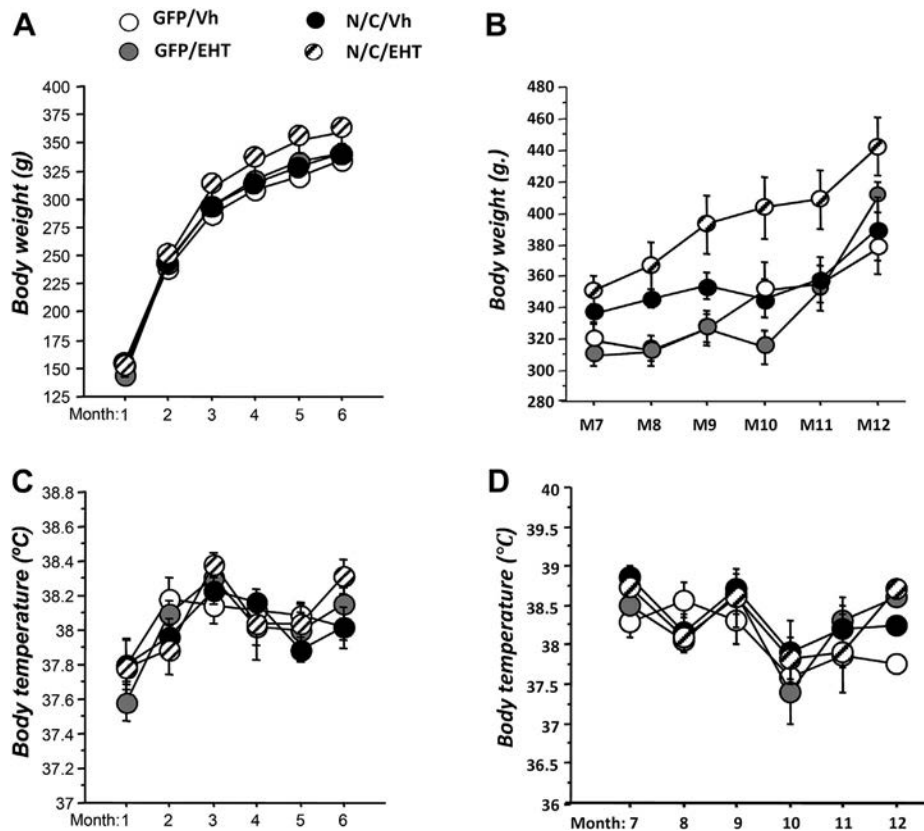
Fig. 4. Effect of eicosanoyl-5-hydroxytryptamide (EHT) treatment on body weight and temperature. Follow-up of body weight and body temperature during the treatment with EHT (A and B, during the first 6 months; C and D, during the last 6 months). Across months, we observed a general increase of the body weight (Fig. 4A and C, analyses of variance [ANOVAs], $p < 0.001$) and of the body temperature (Fig. 4D and E, ANOVAs, $p < 0.001$). But, we did not observe any significant effect of adenoassociated virus (AAV)-$I_{2NTF/CTF}$ infection or EHT on these parameters (Fig. 4A and C, ANOVAs, $p > 0.141$; Fig. 4B and D, ANOVAs, $p > 0.263$) during the period of the treatment.
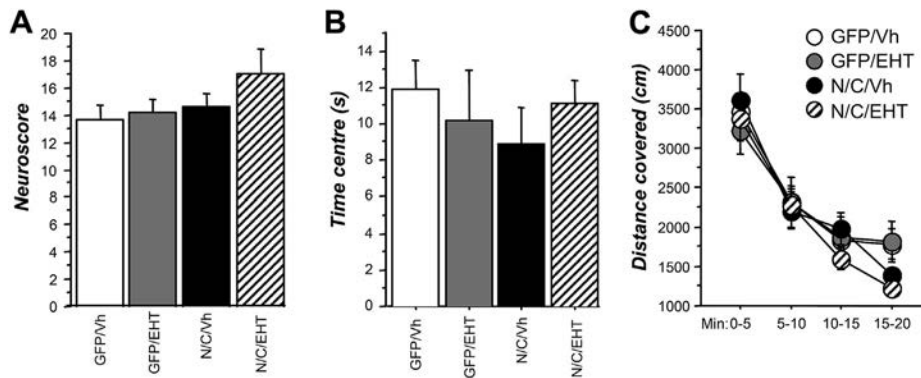
Fig. 5. General behavior in 6-month-old rats. (A) Assessment of neurologic examination (see Supplementary Table S1) quantitated as neuroscore. (B) Anxiety measured by time spent by an animal in the center of the arena. (C) Exploratory activity measured by distance covered exploring the arena. Eicosanoyl-5-hydroxytryptamide (EHT) treatment had no significant effect on any of the previously mentioned measures of general behavior.

3.4. Evaluation after 6 months of treatment with EHT

Figure 5A represents the neuroscore. Statistical analysis of data obtained from the assessment of neurologic examination did not reveal any significant difference among groups (Fig. 5A, Kruskal-Wallis test, $p = 0.380$). This result indicates that, at 6 months of age, AAV-$I_{2NTF/CTF}$ rats did not present any impairment in neurologic function and that treatment with EHT did not induce any neurologic side effects.

As shown in Fig. 5B, there was a tendency for AAV-$I_{2NTF/CTF}$ (N/C/vh) rats to visit less the center of the arena than other groups. But statistical analysis did not reveal any significant difference (Fig. 5B, ANOVA, $p = 0.736$) among groups. This tendency to explore less the center of the open field suggested that, as the pathology develops in AAV-$I_{2NTF/CTF}$ rats, anxiety levels would shift toward hyperanxiety. However, treatment with EHT restored anxiety to normal levels.

During the 20 minutes of free exploration, all groups covered similar distance (Fig. 5C, ANOVA, $p = 0.852$), suggesting that all animals displayed similar level of exploration. No effect of the treatment was observed.

3.5. Evaluation after 12 months of treatment with EHT

Figure 6A represents performance of rats in the hind-limb extension reflex test. Statistical analysis did not reveal any difference between groups (Fig. 6A, Student t tests, $p > 0.059$). This result indicates that, at 12 months of age, AAV-$I_{2NTF/CTF}$ rats did not present any deterioration of peripheral neurologic functions and that treatment with EHT did not induce any peripheral neurologic side effects.

As shown in Fig. 6B, statistical analysis did not reveal any significant difference between groups in the prehensile traction test (Fig. 6B, Student t tests, $p > 0.200$). As represented in the regression chart, correlation analysis of the body weight and the prehensile traction score of the animals did not show any significant effect between body weight and performance in the test (Fig. 6C). These results indicate that neither the AAV-$I_{2NTF/CTF}$ infection nor the treatment with EHT induced any changes in forelimb muscle strength.

Finally, Fig. 6D–G represents analysis of different parameters for the footprint test. Statistical analysis did not reveal any difference between groups in any parameter (Fig. 6D–G, Student t tests, $p > 0.528$). These analyses showed that neither the AAV-$I_{2NTF/CTF}$ infection nor the treatment with EHT altered motor coordination and synchrony.

3.6. Dietary supplementation with EHT blocks I_2^{PP2A} inhibition of PP2A and prevents tau hyperphosphorylation

I_2-N/C fragments are known to bind to PP2Ac and inhibit phosphatase activity (Arnaud et al., 2011). We therefore compared the levels of PP2A activity toward phospho-tau in the brains of rats raised with and without dietary EHT supplementation. On normal diets, PP2A activity was significantly lower in rats that express I_2-N/C than in GFP controls. EHT dietary supplementation completely rescued the I_2-N/C–induced PP2A deficiency (Fig. 7A and B). Neither I_2-N/C expression nor EHT treatment caused any significant changes in the level of total PP2Ac protein. These data confirm that expression of I_2-N/C inhibits PP2A activity and that treatment with EHT can block I_2-N/C–induced PP2A inhibition.

The principal form of PP2A that dephosphorylates phospho-tau requires carboxy methylation at its C-terminus (Tolstykh et al., 2000; Wu et al., 2000). Levels of PP2A methylation are controlled by a balance between the activities of 2 highly conserved PP2A-specific enzymes: a methyl transferase, PPMT, that transfers methyl groups from S-adenosylmethionine to the PP2A carboxy terminus and a methyl esterase, PME, that demethylates PP2A. EHT was initially identified as a component in coffee extracts that inhibited the PP2A demethylation reaction (Lee et al., 2013). Dramatic increases in PP2A demethylation have been observed in brains from AD patients (Sontag et al., 2004). The effect of EHT on levels of PP2A methylation in I_2-N/C and control rats was therefore investigated, and it was found that EHT treatment significantly reduced the levels of demethylated PP2Ac in I_2-N/C rats; a similar trend was seen in GFP controls (Fig. 7C and D). Together, these data suggest that the expression of I_2-N/C decreases PP2A activity and that the treatment with EHT that blocks PP2A demethylation (Lee et al., 2011) can rescue the I_2-N/C inhibition of phosphatase activity.

Because PP2A is the major brain phospho-tau phosphatase (Bennecib et al., 2000; Gong et al., 2000; Liu et al., 2005), I_2-N/C inhibition of PP2A activity would be expected to cause tau hyperphosphorylation. Western blot analysis of tau phosphorylation confirmed this supposition. I_2-N/C expression significantly decreased the total tau level and increased tau hyperphosphorylation compared with GFP control animals at T205, T212, S214, S262/356, and S396, but not at S199, a PP2A nonpreferred site (Liu et al., 2005) (Fig. 8). Treatment with EHT reduced I_2-N/C–induced tau hyperphosphorylation at most of these sites; there were no significant differences between EHT-treated experimental and GFP control rats. These results indicate that I_2-N/C expression induces abnormal hyperphosphorylation of tau through inhibition
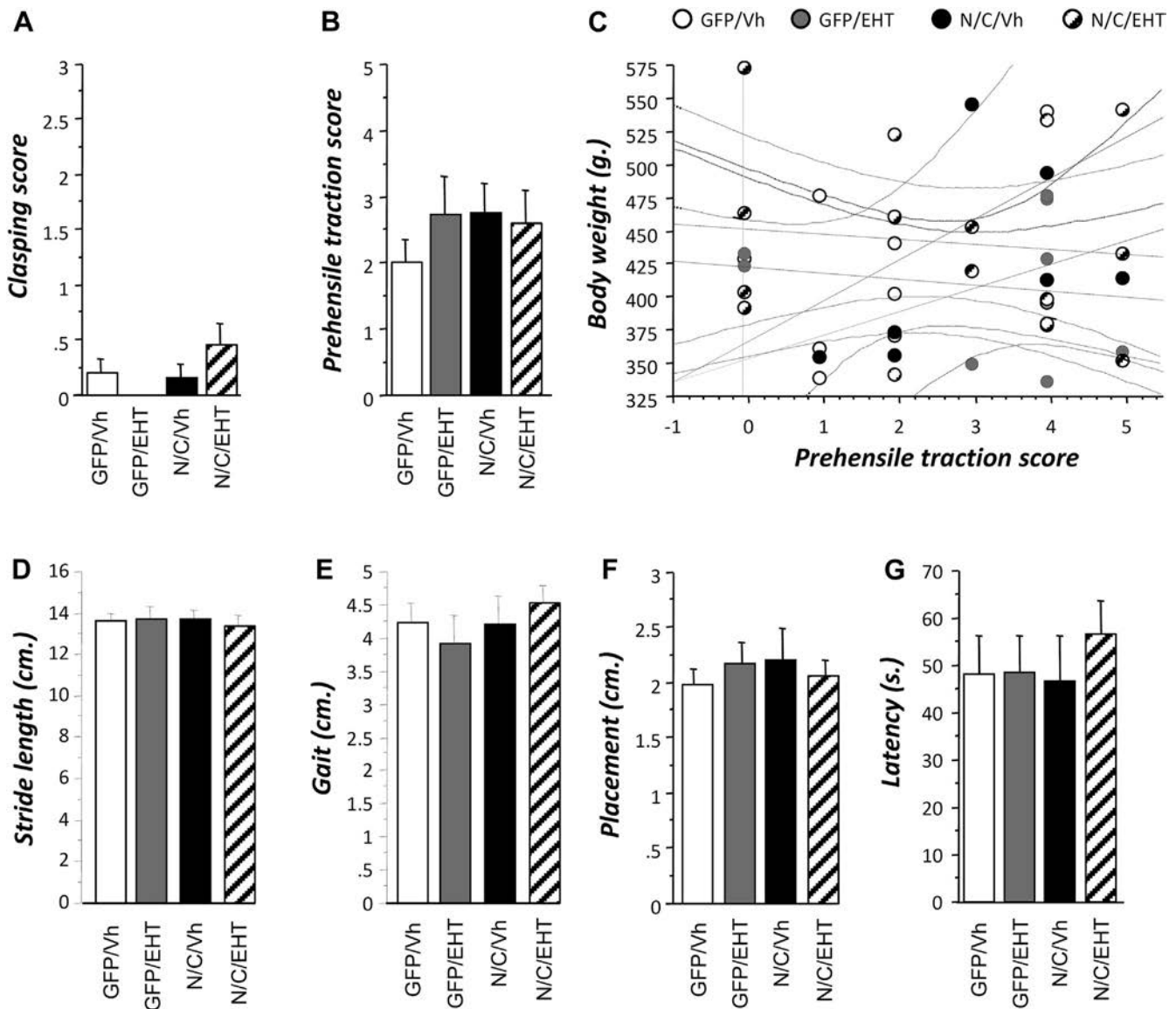
Fig. 6. Lack of any side effects in eicosanoyl-5-hydroxytryptamide (EHT)–treated and control-treated rats at 12 months of age. Different tasks corresponding to general behavior performed at 12 months of age in the 4 groups of rats. (A) Clasping reflex score. (B and C) Prehensile traction score. (D–F) Stride length, gait, and placement in footprint test. (G) Latency to explore novel object in an arena in neophobia test. No significant differences among the 4 groups of animals were found in any of the previously mentioned general behavioral tests, indicating no adverse effect of EHT treatment.

of PP2A activity and that treatment with EHT ameliorates this pathology.

PP2A activity and the levels of tau hyperphosphorylation are known to have a negative correlation at the phosphorylation sites most associated with pathology in AD brain (Liu et al., 2005). As shown in Figs. 7 and 8, PP2A activity was significantly decreased in I_2-N/C rats, tau hyperphosphorylation was coordinately increased, and both the changes in PP2A and tau phosphorylation were rescued in EHT-treated animals. To further establish that the hyperphosphorylation of tau that was observed in I_2-N/C rats in the present study was because of the inhibition of PP2A activity, we evaluated this possibility with Spearman nonparametric correlation analysis. We found a significant negative correlation between the PP2A activity and the abnormal hyperphosphorylation of tau at T205 ($p = 0.0307$), T212 ($p = 0.046$), S262/356 ($p = 0.0002$), S396 ($p = 0.0064$), and S396/404 ($p = 0.0434$) (Fig. 8). These data strongly support the hypothesis that EHT prevented I_2-N/T-induced hyperphosphorylation of tau by maintaining

healthy levels of active PP2A in the presence of overexpressed I_2-N/C.

3.7. EHT treatment reduces intraneuronal Aβ accumulation

Reduced levels of PP2A activity induced by I_2-N/C (Bolognin et al., 2012) and by other means (Sontag et al., 2007) have previously been shown to lead to increases in Aβ load. The effect of EHT treatment on the accumulation of intraneuronal Aβ in I_2-N/C rats was therefore investigated. The immunohistochemical analysis revealed a low number of intraneuronal Aβ-positive cells in rats treated with EHT compared with nontreated rats (Fig. 9). These results suggest that I_2-N/C expression promotes the amyloidogenic processing of APP and that this effect can be rescued by EHT treatment. Our findings, though preliminary, are in agreement with those of Sontag et al. (2007) who showed that increase in PP2A activity can lead to nonamyloidogenic processing of APP.
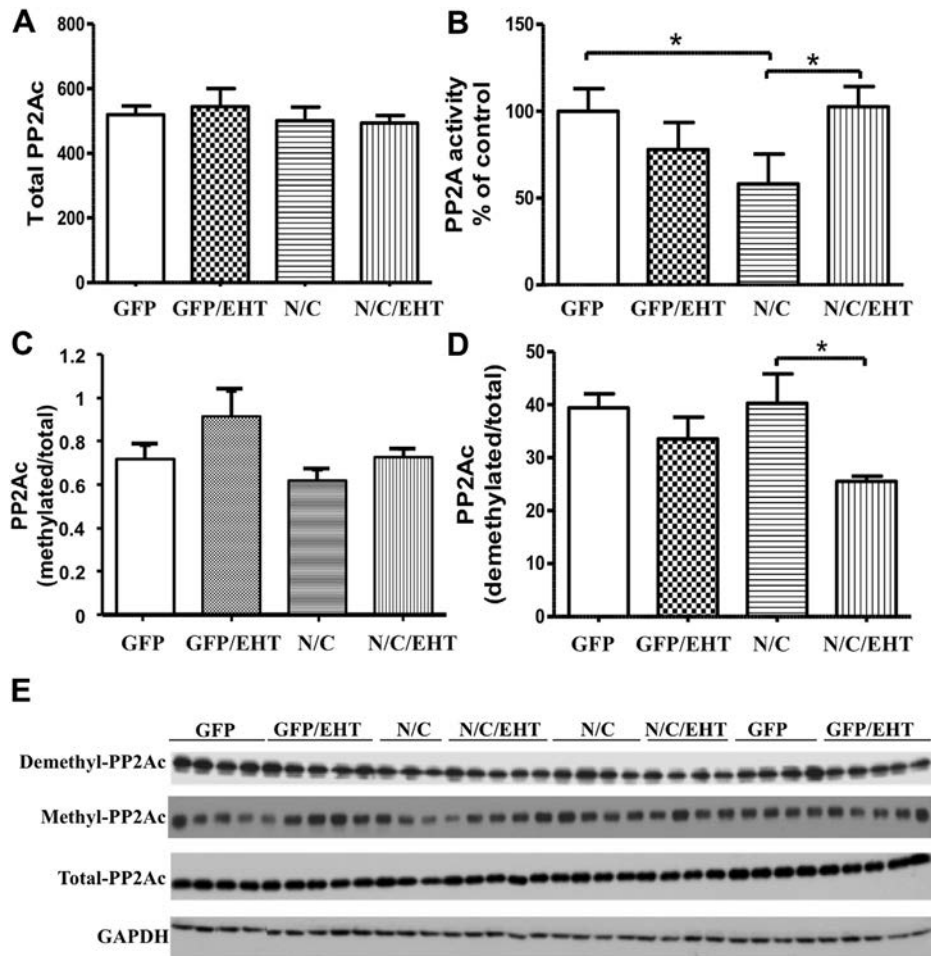
Fig. 7. Eicosanoyl-5-hydroxytryptamide (EHT) increases phosphoprotein phosphatase 2A (PP2A) activity in I_2^{PP2A} N- and C-terminal fragments (I_2-N/C) rats. (A) Western blot quantification of I_2-N/C and green fluorescent protein (GFP) rat hippocampi showing the effect of EHT treatment on the level of total PP2A catalytic subunit (PP2Ac). (B) PP2A activity was recovered in I_2-N/C rats treated with EHT, evaluated by PP2A phosphatase assay. (C) EHT increased PP2Ac methylation and (D) reduced PP2Ac demethylation in I_2-N/C rats. (E) Representative blots shown for demethylated (1D6), methylated (4D9), and total PP2Ac (6A3) and glyceraldehyde 3-phosphate dehydrogenase (GAPDH). * $p < 0.05$. The data are shown as mean ± standard error, normalized by GAPDH for total PP2A.

4. Discussion

AD is multifactorial and involves several different etiopathogenic mechanisms (Iqbal et al., 2005b). The familial form, which accounts for <1%, and the sporadic form, which represents the remaining >99% of the cases of AD, are histopathologically identical. Although the familial form of AD has been associated with certain mutations in APP and presenilins 1 and 2, and the inheritance of the *APOE4* allele markedly increases the risk for the disease, the causes of the sporadic form of the disease are not understood. Nevertheless, the decrease of PP2A activity associated with an increase in the expression, the cleavage and the translocation of I_2^{PP2A}, and a decrease in the methylation of PP2Ac reported in AD brain (Bolognin et al., 2012; Gong et al., 1993, 1995; Sontag et al., 2004; Tanimukai et al., 2005; Wang et al., 2010) can lead both to tau and Aβ pathologies. The present study shows that the overexpression and cleavage of I_2^{PP2A} can lead to increases in PP2Ac demethylation, inhibition of PP2A activity, tau hyperphosphorylation, Aβ expression, and cognitive impairment and that all these changes are significantly reversed by a minor component of coffee, EHT.

The AAV1-$I_{2NTF-CTF}$ rat model used in the present study was developed in our laboratory (Bolognin et al., 2012). Compared with transgenic animals, one of the major advantages of the

viral gene transfer technology used to generate the I_2-N/C rat model is that long-term transgene expression is achieved without affecting the genetic background of the animal (Lawlor et al., 2007). Rats injected with AAV serotype 1 vector encoding the 2 fragments of I_2^{PP2A} showed a marked reduction of PP2A activity beginning at 4 months of age (Bolognin et al., 2012). The present study extended these findings to 13 months of age, when the cytosolic tau and Aβ pathologies were evident, making this model appropriate to study the effect of changes in PP2A activity on AD-type changes. EHT was administered to rats from the age of 21 days to 13 months. Compared with nontreated animals, a decrease in demethylation of PP2Ac was observed in EHT-treated rats, indicating the efficacy of the compound over chronic long-term use. These results corroborate previous reports showing EHT efficacy in both attenuation of α-synucleinopathies in vivo after a 9-month treatment and inhibition of PP2A demethylation in vitro (Lee et al., 2011). Pharmacokinetic studies delivering [^{3}H]-EHT intraperitoneally revealed that this compound crosses the blood brain barrier achieving levels sufficient to inhibit PP2A demethylation, indicating its feasibility for proof of concept studies (Lee et al., 2011). EHT was identified as the major PP2A demethylation inhibitor in coffee (Lee et al., 2011) and was reported to be effective in preclinical studies (Lee et al., 2011, 2013).
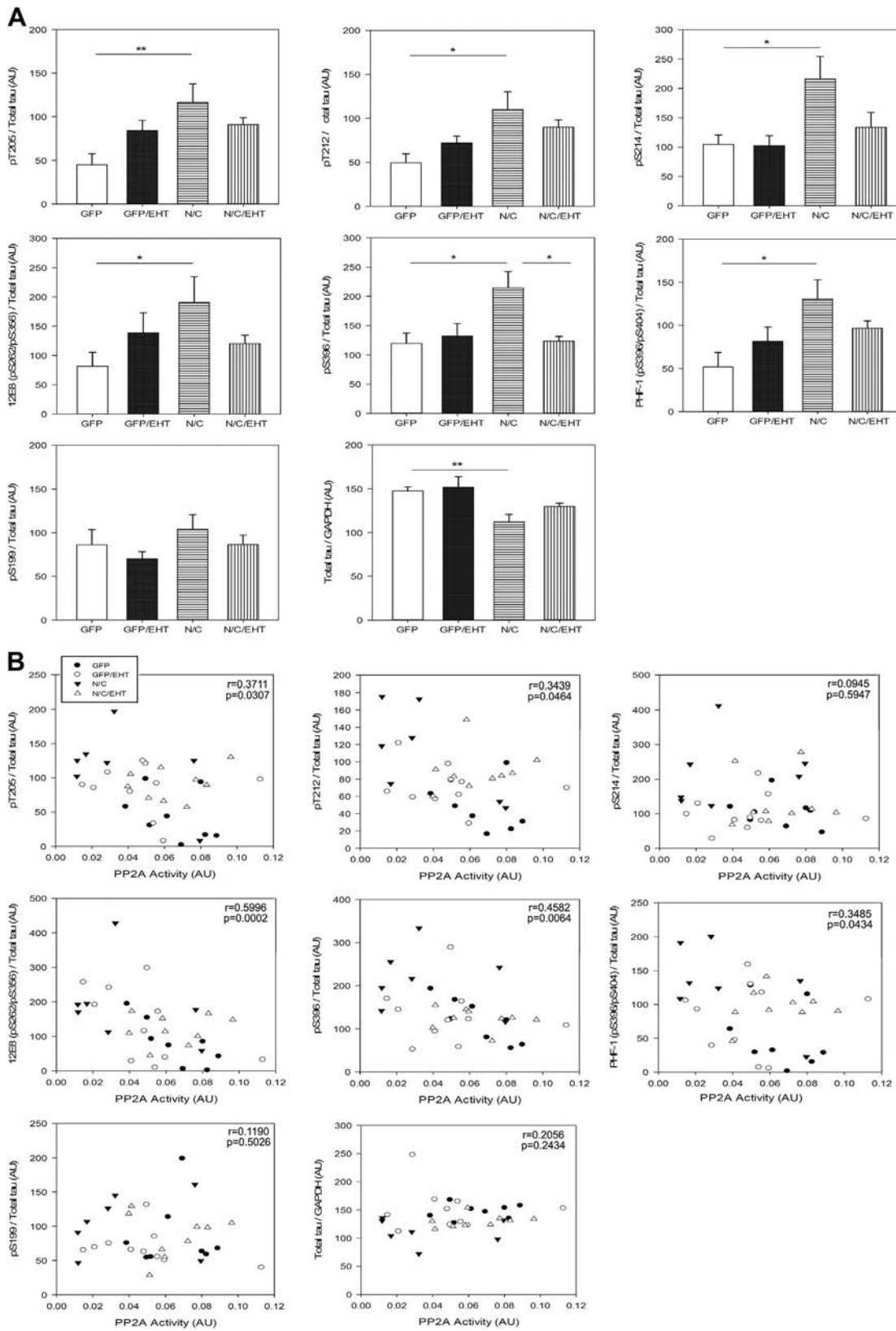
Fig. 8. Abnormal hyperphosphorylation of tau in rats expressing I_2^{PP2A} N- and C-terminal fragments (I_2-N/C) is prevented by eicosanoyl-5-hydroxytryptamide (EHT) treatment. (A) Western blot density data are shown as mean ± standard error, normalized by glyceraldehyde 3-phosphate dehydrogenase (GAPDH) and for all the phosphorylated sites by total tau. * $p < 0.05$ and ** $p < 0.01$. (B) Phosphoprotein phosphatase 2A (PP2A) activity values from the 4 groups of rats were correlated with the values corresponding to the densitometry analysis of Western blots developed for various tau-phospho sites. Decrease in hyperphosphorylation of tau at Thr205, Thr212, Ser262/356 (12E8 site), and Ser396/404 (PHF-1 site) directly correlated with increase in PP2A activity.
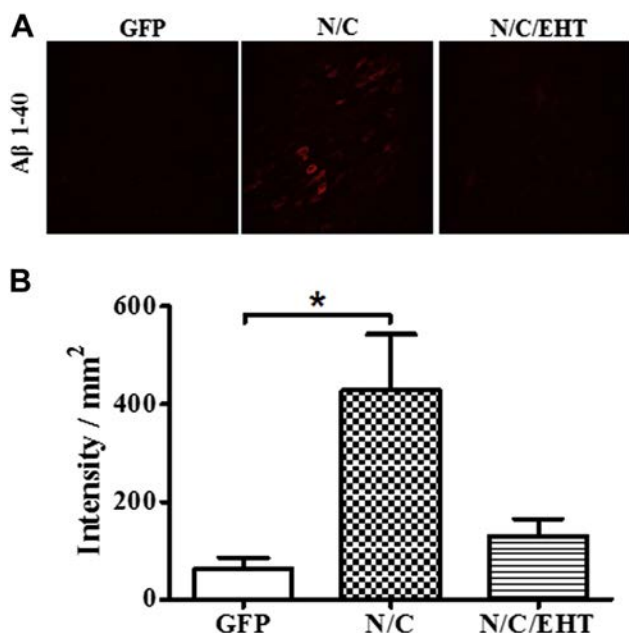
Fig. 9. I_2^{PP2A} N- and C-terminal fragments (I_2-N/C) overexpression increases intraneuronal amyloid β ($A\beta$)$_{1-40}$ load, which appears to be attenuated by eicosanoyl-5-hydroxytryptamide (EHT). (A) Representative micrographs of immunohistochemistry (IHC) from cerebral cortex showed $A\beta_{1-40}$ load increases in I_2-N/C-treated ($p < 0.05$, $n = 3$) but not EHT-treated rats. (B) IHC quantification of I_2-N/C and green fluorescent protein (GFP) rat hippocampi showing the effect of EHT treatment on the level of $A\beta_{1-40}$. EHT treatment appears to attenuate the Aβ pathology ($p = 0.1$, $n = 3$ animals per group; $p < 0.01$ for $n = 12$ sections from 3 animals per group). *$p < 0.05$.

Epidemiologic studies have established a negative correlation between coffee consumption and the incidence of Parkinson's disease and AD (Barranco Quintana et al., 2007; Saaksjarvi et al., 2008). In the present study, we observed that rats expressing I_2-N/C displayed increased PP2A demethylation and a decrease in PP2A activity and that treatment with EHT decreased PP2A demethylation and increased PP2A activity toward tau. Previous studies showed that methylation of PP2Ac affects phosphatase activity in part by facilitating the binding of the regulatory Bα subunits to AC dimers (Tolstykh et al., 2000; Xu et al., 2008). It is not clear, however, that the protective effects of EHT against I_2^{PP2A} inhibition derive entirely from inhibition of PP2A demethylation. The inhibitory effect of EHT on demethylation most likely stems from formation of a complex between EHT and PP2A that precludes the interaction between PME and PP2A that is required for demethylation. Thus, the possibility cannot be excluded that the EHT/PP2A complex may also preclude the formation of inhibitory complexes between PP2A and I_2^{PP2A} in much the same way that it appears to block the interaction between PP2A and PME.

As a consequence of the decrease in PP2A activity in $I_{2NTF-CTF}$ rats, we observed a clear increase in tau hyperphosphorylation at multiple sites. The association between these events was confirmed by correlation analysis, showing that decreases in PP2A activity are negatively correlated with the hyperphosphorylation of tau at several sites, particularly the PP2A-dependent sites S262, T212, T205, and S396. S199 and S214 that are not preferred sites for PP2A did not show any correlation. This analysis is consistent with previous reports in AD cases (Liu et al., 2005). PP2A regulates phosphorylation of tau both directly and by regulating the activities of several tau protein kinases (Iqbal et al., 2005a). The effect of I_2-N/C can be either direct by inhibiting the PP2A activity as we previously demonstrated (Arnaud et al., 2011) or through a downregulation of Bα subunit PP2A holoenzyme that specifically regulates the phosphorylation of tau (Sontag et al., 2007; Xu et al., 2008).

In addition to tau pathology, we also observed an accumulation of intraneuronal Aβ in I_2-N/C rats, which was attenuated in animals treated with EHT. These beneficial effects of EHT treatment may target early Aβ pathologic mechanisms through an increase in PP2A activity. PP2A demethylation, for instance, has been reported to be associated with a concomitant decrease in the steady-state release of neuroprotective APPα phosphorylated species and increased secretion of β- and γ-secretase–cleaved APP fragments, inducing a shift in APP processing toward the amyloidogenic pathway (Sontag et al., 2007). Increased APP phosphorylation, either directly through decreased activity of PP2A toward phospho-APP or indirectly through reduced phosphatase activity toward phospho-JNK, can result in increased Aβ production (Colombo et al., 2009). Thus, activation of PP2A by small molecules such as EHT, offers a new therapeutic approach for the prevention and treatment of AD and other neurodegenerative disorders, including tauopathies such as frontotemporal dementias (Voronkov et al., 2011).

Disclosure statement

Conflicts of interest disclosure: Signum Biosciences has a US patent on the EHT compound used for this study. The animal studies conform to National Institutes of Health guidelines and were approved by our institutional Institutional Animal Care and Use Committee.

Appendix A. Supplementary data

Supplementary data associated with this article can be found, in the online version, at http://dx.doi.org/10.1016/j.neurobiolaging.2014.06.012.

References

Alonso, A.D., Zaidi, T., Grundke-Iqbal, I., Iqbal, K., 1994. Role of abnormally phosphorylated tau in the breakdown of microtubules in Alzheimer disease. Proc. Natl. Acad. Sci. U.S.A 91, 5562–5566.

Alonso, A.D., Di Clerico, J., Li, B., Corbo, C.P., Alaniz, M.E., Grundke-Iqbal, I., Iqbal, K., 2010. Phosphorylation of tau at thr212, thr231, and ser262 combined causes neurodegeneration. J. Biol. Chem. 285, 30851–30860.

Arnaud, L., Chen, S., Liu, F., Li, B., Khatoon, S., Grundke-Iqbal, I., Iqbal, K., 2011. Mechanism of inhibition of pp2a activity and abnormal hyperphosphorylation of tau by i(2)(pp2a)/set. FEBS Lett. 585, 2653–2659.

Bancher, C., Brunner, C., Lassmann, H., Budka, H., Jellinger, K., Wiche, G., Seitelberger, F., Grundke-Iqbal, I., Iqbal, K., Wisniewski, H.M., 1989. Accumulation of abnormally phosphorylated tau precedes the formation of neurofibrillary tangles in Alzheimer's disease. Brain Res. 477, 90–99.

Barranco Quintana, J.L., Allam, M.F., Serrano Del Castillo, A., Fernandez-Crehuet Navajas, R., 2007. Alzheimer's disease and coffee: a quantitative review. Neurol. Res. 29, 91–95.

Bennecib, M., Gong, C., Wegiel, J., Lee, M.H., Grundke-Iqbal, I., Iqbal, K., 2000. Inhibition of protein phosphatases and regulation of tau phosphorylation in rat brain. Alzheimer's Rep. 3, 295–304.

Bensadoun, A., Weinstein, D., 1976. Assay of proteins in the presence of interfering materials. Anal. Biochem. 70, 241–250.

Bolognin, S., Blanchard, J., Wang, X., Basurto-Islas, G., Tung, Y.C., Kohlbrenner, E., Grundke-Iqbal, I., Iqbal, K., 2012. An experimental rat model of sporadic Alzheimer's disease and rescue of cognitive impairment with a neurotrophic peptide. Acta Neuropathol. 123, 133–151.

Cataldo, A.M., Petanceska, S., Terio, N.B., Peterhoff, C.M., Durham, R., Mercken, M., Mehta, P.D., Buxbaum, J., Haroutunian, V., Nixon, R.A., 2004. Abeta localization

in abnormal endosomes: association with earliest abeta elevations in AD and Down syndrome. Neurobiol. Aging 25, 1263–1272.

Chohan, M.O., Khatoon, S., Iqbal, I.G., Iqbal, K., 2006. Involvement of i2pp2a in the abnormal hyperphosphorylation of tau and its reversal by memantine. FEBS Lett. 580, 3973–3979.

Colombo, A., Bastone, A., Ploia, C., Sclip, A., Salmona, M., Forloni, G., Borsello, T., 2009. Jnk regulates app cleavage and degradation in a model of Alzheimer's disease. Neurobiol. Dis. 33, 518–525.

Espana, J., Gimenez-Llort, L., Valero, J., Minano, A., Rabano, A., Rodriguez-Alvarez, J., LaFerla, F.M., Saura, C.A., 2010. Intraneuronal beta-amyloid accumulation in the amygdala enhances fear and anxiety in Alzheimer's disease transgenic mice. Biol. Psychiatry 67, 513–521.

Gandy, S., Simon, A.J., Steele, J.W., Lublin, A.L., Lah, J.J., Walker, L.C., Levey, A.I., Krafft, G.A., Levy, E., Checler, F., Glabe, C., Bilker, W.B., Abel, T., Schmeidler, J., Ehrlich, M.E., 2010. Days to criterion as an indicator of toxicity associated with human Alzheimer amyloid-beta oligomers. Ann. Neurol. 68, 220–230.

Gong, C.X., Singh, T.J., Grundke-Iqbal, I., Iqbal, K., 1993. Phosphoprotein phosphatase activities in Alzheimer disease brain. J. Neurochem. 61, 921–927.

Gong, C.X., Shaikh, S., Wang, J.Z., Zaidi, T., Grundke-Iqbal, I., Iqbal, K., 1995. Phosphatase activity toward abnormally phosphorylated tau: decrease in Alzheimer disease brain. J. Neurochem. 65, 732–738.

Gong, C.X., Lidsky, T., Wegiel, J., Zuck, L., Grundke-Iqbal, I., Iqbal, K., 2000. Phosphorylation of microtubule-associated protein tau is regulated by protein phosphatase 2a in mammalian brain. Implications for neurofibrillary degeneration in Alzheimer's disease. J. Biol. Chem. 275, 5535–5544.

Grundke-Iqbal, I., Iqbal, K., Quinlan, M., Tung, Y.C., Zaidi, M.S., Wisniewski, H.M., 1986a. Microtubule-associated protein tau. A component of Alzheimer paired helical filaments. J. Biol. Chem. 261, 6084–6089.

Grundke-Iqbal, I., Iqbal, K., Tung, Y.C., Quinlan, M., Wisniewski, H.M., Binder, L.I., 1986b. Abnormal phosphorylation of the microtubule-associated protein tau (tau) in Alzheimer cytoskeletal pathology. Proc. Natl. Acad. Sci. U.S.A 83, 4913–4917.

Grundke-Iqbal, I., Vorbrodt, A.W., Iqbal, K., Tung, Y.C., Wang, G.P., Wisniewski, H.M., 1988. Microtubule-associated polypeptides tau are altered in Alzheimer paired helical filaments. Brain Res. 464, 43–52.

Grundke-Iqbal, I., Iqbal, K., George, L., Tung, Y.C., Kim, K.S., Wisniewski, H.M., 1989. Amyloid protein and neurofibrillary tangles coexist in the same neuron in Alzheimer disease. Proc. Natl. Acad. Sci. U.S.A 86, 2853–2857.

Henckaerts, E., Dutheil, N., Zeltner, N., Kattman, S., Kohlbrenner, E., Ward, P., Clement, N., Rebollo, P., Kennedy, M., Keller, G.M., Linden, R.M., 2009. Site-specific integration of adeno-associated virus involves partial duplication of the target locus. Proc. Natl. Acad. Sci. U.S.A 106, 7571–7576.

Iqbal, K., Grundke-Iqbal, I., Zaidi, T., Merz, P.A., Wen, G.Y., Shaikh, S.S., Wisniewski, H.M., Alafuzoff, I., Winblad, B., 1986. Defective brain microtubule assembly in Alzheimer's disease. Lancet 2, 421–426.

Iqbal, K., Alonso, A., Chen, S., Chohan, M.O., El-Akkad, E., Gong, C.X., Khatoon, S., Li, B., Liu, F., Rahman, A., Tanimukai, H., Grundke-Iqbal, I., 2005a. Tau pathology in Alzheimer disease and other tauopathies. Biochim. Biophys. Acta 1739, 198–210.

Iqbal, K., Flory, M., Khatoon, S., Soininen, H., Pirttila, T., Lehtovirta, M., Alafuzoff, I., Blennow, K., Andreasen, N., Vanmechelen, E., Grundke-Iqbal, I., 2005b. Subgroups of Alzheimer's disease based on cerebrospinal fluid molecular markers. Ann. Neurol. 58, 748–757.

Klein, W.L., 2002. Abeta toxicity in Alzheimer's disease: globular oligomers (addls) as new vaccine and drug targets. Neurochem. Int. 41, 345–352.

Kopke, E., Tung, Y.C., Shaikh, S., Alonso, A.C., Iqbal, K., Grundke-Iqbal, I., 1993. Microtubule-associated protein tau. Abnormal phosphorylation of a non-paired helical filament pool in Alzheimer disease. J. Biol. Chem. 268, 24374–24384.

Korenova, M., Zilka, N., Stozicka, Z., Bugos, O., Vanicky, I., Novak, M., 2009. Neuroscale, the battery of behavioral tests with novel scoring system for phenotyping of transgenic rat model of tauopathy. J. Neurosci. Methods 177, 108–114.

Lawlor, P.A., Bland, R.J., Das, P., Price, R.W., Holloway, V., Smithson, L., Dicker, B.L., During, M.J., Young, D., Golde, T.E., 2007. Novel rat Alzheimer's disease models based on aav-mediated gene transfer to selectively increase hippocampal abeta levels. Mol. Neurodegener. 2, 11.

Lee, K.W., Chen, W., Junn, E., Im, J.Y., Grosso, H., Sonsalla, P.K., Feng, X., Ray, N., Fernandez, J.R., Chao, Y., Masliah, E., Voronkov, M., Braithwaite, S.P., Stock, J.B., Mouradian, M.M., 2011. Enhanced phosphatase activity attenuates alpha-synucleinopathy in a mouse model. J. Neurosci. 31, 6963–6971.

Lee, K.W., Im, J.Y., Woo, J.M., Grosso, H., Kim, Y.S., Cristovao, A.C., Sonsalla, P.K., Schuster, D.S., Jalbut, M.M., Fernandez, J.R., Voronkov, M., Junn, E., Braithwaite, S.P., Stock, J.B., Mouradian, M.M., 2013. Neuroprotective and anti-inflammatory properties of a coffee component in the mptp model of Parkinson's disease. Neurotherapeutics 10, 143–153.

Li, M., Guo, H., Damuni, Z., 1995. Purification and characterization of two potent heat-stable protein inhibitors of protein phosphatase 2a from bovine kidney. Biochemistry 34, 1988–1996.

Li, M., Makkinje, A., Damuni, Z., 1996. The myeloid leukemia-associated protein set is a potent inhibitor of protein phosphatase 2a. J. Biol. Chem. 271, 11059–11062.

Liu, F., Grundke-Iqbal, I., Iqbal, K., Gong, C.X., 2005. Contributions of protein phosphatases pp1, pp2a, pp2b and pp5 to the regulation of tau phosphorylation. Eur. J. Neurosci. 22, 1942–1950.

Malkova, L., Mishkin, M., 2003. One-trial memory for object-place associations after separate lesions of hippocampus and posterior parahippocampal region in the monkey. J. Neurosci. 23, 1956–1965.

Masters, C.L., Simms, G., Weinman, N.A., Multhaup, G., McDonald, B.L., Beyreuther, K., 1985. Amyloid plaque core protein in Alzheimer disease and Down syndrome. Proc. Natl. Acad. Sci. U.S.A 82, 4245–4249.

Mori, C., Spooner, E.T., Wisniewsk, K.E., Wisniewski, T.M., Yamaguch, H., Saido, T.C., Tolan, D.R., Selkoe, D.J., Lemere, C.A., 2002. Intraneuronal abeta42 accumulation in Down syndrome brain. Amyloid 9, 88–102.

Morris, R.G., Garrud, P., Rawlins, J.N., O'Keefe, J., 1982. Place navigation impaired in rats with hippocampal lesions. Nature 297, 681–683.

Oddo, S., Caccamo, A., Shepherd, J.D., Murphy, M.P., Golde, T.E., Kayed, R., Metherate, R., Mattson, M.P., Akbari, Y., LaFerla, F.M., 2003. Triple-transgenic model of Alzheimer's disease with plaques and tangles: intracellular abeta and synaptic dysfunction. Neuron 39, 409–421.

Riedel, G., Micheau, J., Lam, A.G., Roloff, E.L., Martin, S.J., Bridge, H., de Hoz, L., Poeschel, B., McCulloch, J., Morris, R.G., 1999. Reversible neural inactivation reveals hippocampal participation in several memory processes. Nat. Neurosci. 2, 898–905.

Saaksjarvi, K., Knekt, P., Rissanen, H., Laaksonen, M.A., Reunanen, A., Mannisto, S., 2008. Prospective study of coffee consumption and risk of Parkinson's disease. Eur. J. Clin. Nutr. 62, 908–915.

Santacruz, K., Lewis, J., Spires, T., Paulson, J., Kotilinek, L., Ingelsson, M., Guimaraes, A., DeTure, M., Ramsden, M., McGowan, E., Forster, C., Yue, M., Orne, J., Janus, C., Mariash, A., Kuskowski, M., Hyman, B., Hutton, M., Ashe, K.H., 2005. Tau suppression in a neurodegenerative mouse model improves memory function. Science 309, 476–481.

Seubert, P., Mawal-Dewan, M., Barbour, R., Jakes, R., Goedert, M., Johnson, G.V., Litersky, J.M., Schenk, D., Lieberburg, I., Trojanowski, J.Q., Lee, V. M-Y., 1995. Detection of phosphorylated ser262 in fetal tau, adult tau, and paired helical filament tau. J. Biol. Chem. 270, 18917–18922.

Sontag, E., Hladik, C., Montgomery, L., Luangpirom, A., Mudrak, I., Ogris, E., White III, C.L., 2004. Downregulation of protein phosphatase 2a carboxyl methylation and methyltransferase may contribute to Alzheimer disease pathogenesis. J. Neuropathol. Exp. Neurol. 63, 1080–1091.

Sontag, E., Nunbhakdi-Craig, V., Sontag, J.M., Diaz-Arrastia, R., Ogris, E., Dayal, S., Lentz, S.R., Arning, E., Bottiglieri, T., 2007. Protein phosphatase 2a methyltransferase links homocysteine metabolism with tau and amyloid precursor protein regulation. J. Neurosci. 27, 2751–2759.

Tanaka, T., Zhong, J., Iqbal, K., Trenkner, E., Grundke-Iqbal, I., 1998. The regulation of phosphorylation of tau in sy5y neuroblastoma cells: the role of protein phosphatases. FEBS Lett. 426, 248–254.

Tanimukai, H., Grundke-Iqbal, I., Iqbal, K., 2005. Up-regulation of inhibitors of protein phosphatase-2a in Alzheimer's disease. Am. J. Pathol. 166, 1761–1771.

Tolstykh, T., Lee, J., Vafai, S., Stock, J.B., 2000. Carboxyl methylation regulates phosphoprotein phosphatase 2a by controlling the association of regulatory b subunits. EMBO J. 19, 5682–5691.

Tsujio, I., Zaidi, T., Xu, J., Kotula, L., Grundke-Iqbal, I., Iqbal, K., 2005. Inhibitors of protein phosphatase-2a from human brain structures, immunocytological localization and activities towards dephosphorylation of the Alzheimer type hyperphosphorylated tau. FEBS Lett. 579, 363–372.

Voronkov, M., Braithwaite, S.P., Stock, J.B., 2011. Phosphoprotein phosphatase 2a: a novel druggable target for Alzheimer's disease. Future Med. Chem. 3, 821–833.

Wang, X., Blanchard, J., Kohlbrenner, E., Clement, N., Linden, R.M., Radu, A., Grundke-Iqbal, I., Iqbal, K., 2010. The carboxy-terminal fragment of inhibitor-2 of protein phosphatase-2a induces Alzheimer disease pathology and cognitive impairment. FASEB J. 24, 4420–4432.

Wong, C.W., Quaranta, V., Glenner, G.G., 1985. Neuritic plaques and cerebrovascular amyloid in Alzheimer disease are antigenically related. Proc. Natl. Acad. Sci. U.S.A 82, 8729–8732.

Wu, J., Tolstykh, T., Lee, J., Boyd, K., Stock, J.B., Broach, J.R., 2000. Carboxyl methylation of the phosphoprotein phosphatase 2a catalytic subunit promotes its functional association with regulatory subunits in vivo. EMBO J. 19, 5672–5681.

Xu, Y., Chen, Y., Zhang, P., Jeffrey, P.D., Shi, Y., 2008. Structure of a protein phosphatase 2a holoenzyme: insights into b55-mediated tau dephosphorylation. Mol. Cell. 31, 873–885.

Zolotukhin, S., Potter, M., Zolotukhin, I., Sakai, Y., Loiler, S., Fraites Jr., T.J., Chiodo, V.A., Phillipsberg, T., Muzyczka, N., Hauswirth, W.W., Flotte, T.R., Byrne, B.J., Snyder, R.O., 2002. Production and purification of serotype 1, 2, and 5 recombinant adeno-associated viral vectors. Methods 28, 158–167.